MECHANISMS OF CORROSION MICROCRACKS NUCLEATION IN 08X18N10T STAINLESS STEEL IN WATER SOLUTIONS AT 275 ^{o}C

Karel Matocha

VÍTKOVICE Research & Development , Ostrava , Czech Rep.

Abstract

Axially loaded, quantitatively stressed standard tension test specimens, 3 mm in diameter, were used for investigating the resistance of austenitic stainless steel 08X18N10T (AISI 321) to stress corrosion cracking initiation. The effect of ionic impurities (Cl^-, SO_4^{2-}, Na^+), high temperature pH, corrosion potential and tensile stress on nucleation of microcracks on a smooth surface of test specimens in water solutions at 275^{o}C were investigated.

The occurence of microcracks has been observed in two narrow intervals of high temperature pH . First one can be found in the region of acid solutions (pH_{275} 1,8 – 4), the second one in the region of alkaline solutions (pH_{275}>9,0). Two main mechanisms responsible for microcracks nucleation will be described.

Introduction

Heat exchange tubes and primary collector bodies are the most stress corrosion exposed parts of WWER 440 steam generators (SG). These components are fabricated of titanium stabilized austenitic stainless steel of type 08X18N10T (AISI 321). It is characterized by high resistance against sensitization (precipitation of chromium carbides $M_{23}C_6$ at grain boundaries) [1].

Transgranular stress corrosion cracking (SCC) in secondary circuit water environment has been observed from time to time in these components. The SCC has been localized into the regions where , due to restricted exchange of bulk environment , increased concentrations of ionic impurities such as Cl^- , Na^+ and SO_4^{2-} has been determined (threaded holes of primary collector body flange) [2,3].

Stress corrosion cracking describes the nucleation and a subcritical crack growth of micro and macro cracks due to simultaneous action of tensile stress , material microstructure and environment. A complete understanding of this phenomenon hence lies in an appreciation of the complex interaction between microstructural conditions, environmental factors and the stress/time history applied to the structure.

Due to the presence of the minor phase particles of type Ti(C,N) and nonmetallic inclusions of type $Ti_4C_2S_2$ and Ti(C,N) in the microstructure of 08X18N10T steel one can assume different corrosion behaviour in comparison with nonstabilized sensitized stainless steels (AISI 304) mainly during the initiation stage of SCC.

Studies of SCC initiation stage in 08X18N10T steel, carried out by laboratory autoclave tests of axially loaded quantitatively stresses standard tension test specimens in deaerated high temperature (operating temperature of SG) water solutions [4,5] ,proved that the determination of conditions for occurence and/or supression of SCC is necessary to divide as follows:

- Determination of conditions for microcrack nucleation on a component surface
- Determination of conditions for subcritical growth of microcrack
- Determination of conditions for subcritical growth of macrocrack

The purpose of this work was to examine the mechanisms responsible for corrosion microcrack nucleation on surfaces of test specimens cutted from WWER 440 SG components fabricated from 08X18N10T steel (heat exchange tubes, primary collector body). The tests were carried out in high temperature (275°C) deaerated water solutions with increased concentrations of ionic impurities such as Cl^- , Na^+ and SO_4^{2-} .

Experimental procedure used for the evaluation of SCC initiation stage

Tension test specimens , 3 mm in diameter , oriented in longitudinal direction and cutted off from the upper part of primary collector body and special test specimens made of WWER 440 SG heat exchange tubes were loaded in stressing frames of the constant strain type (see Fig. 1,2) [6]. Each specimen was loaded to the required stress level and the moving beam then locked in position. All components of the stressing frames were also manufactured from 08X18N10T steel. Stress levels were determined from measurements of strains. Round bar test specimens , 3 mm in diameter, were loaded to the total deformation of 0,2% , 0,65% and 1,7% (see tab. I).

Tab.I - Tensile stresses corresponding at 275°C to the total deformations investigated

Total deformation	Tensile stress σ [MPa]	σ/Y [1]
0,20%	169	0,89
0,65%	211	1,11
1,70%	236	1,24

where Y is a yield stress at 275°C.

Special test specimens made of heat exchange tubes were loaded to the total deformation corresponding to yield stress at 275°C (ε_{tot} = 0,35%).

The entire stressing frames were then subjected to autoclave tests at 275°C in static autoclave ,11 l in volume, in selected deaerated water solutions with increased concentrations of Cl^-,SO_4^{2-}, Na^+.

Post autoclave examinations were carried out by metallographic evaluation of longitudinal sections of a gage length of test specimens using metallographic microscope OLYMPUS. Oxide layer connection and thickness , rate of microcracks occurence and preferential nucleation sites were investigated.

Testing material

All test specimens ,3 mm in diameter, were made from the upper part of the primary collector ,73 mm in thickness, cutted off after 9 years of operation at Dukovany NPP. Ti stabilized austenitic stainless steel of type 08X18N10T (0,073%C, 1,42%Mn, 0,48%Si, 10,9%Ni, 19,1%Cr, 0,010%P, 0,012%S, 0,66%Ti, 0,021%Mo, 0,034%Cu) was used in annealed condition (1050°C/2 hours/water).

Tensile properties at laboratory temperature and at 275°C are summarized in tab.II.

Tab.II - Tensile properties of the steel under investigation
(crosshead speed 0.1mm/min.)

Test Temperature	Yield stress [MPa]	Tensile strength [MPa]	Elongation [%]	Reduction of Area [%]
Laboratory	258	546	65	77
275 °C	202	392	36	72

Austenitic microstructure with a small amount of δ ferrite (~ 2 %) was characterized by grain size ranging from 31 to 44 μm, the presence of minor phase particles of type Ti(C,N) and nonmetallic inclusions of type $Ti_4C_2S_2$ and Ti(C,N) with surface density 96 particles/mm^2.

Tensile properties of WWER 440 heat exchange tubes material at laboratory temperature and at 275^{o}C are summarized in tab. III.

Tab. III Tensile properties of WWER 440 heat exchange tubes material
(crosshead speed 0.1 mm/min.)

Test Temperature	Yield stress [MPa]	Tensile strength [MPa]	Elongation [%]
Laboratory	360	735	47
275°C	303	521	23

In comparison with primary collector body material, tubing material (08X18N10T steel of the same chemical composition) shows significantly higher yield stress and tensile strength. Austenitic microstructure is fine-grained with the average grain size of 22 μm. It is characterized by the presence of minor phase particles of type Ti(C,N) and nonmetallic inclusions of type $Ti_4C_2S_2$ and Ti(C,N) with surface density 123 particles/mm^2.

Significantly lower elongation at SG operating temperature, in comparison with that obtained at laboratory temperature, was observed for both primary collector and tubing material. The literature data show this fact is characteristic for this type of steel [7]. Decrease of elongation at elevated temperatures (≥ 100^{o}C) can be explained by higher hardening exponent n [8], easier interface failure between matrix and nonmetallic inclusions and/or different expansion of nonmetallic inclusions and matrix.

Experimental results

Following the results of the tensile tests at elevated temperature the test specimens axially loaded in stressing frames were , first of all , exposed in air at 275^{o}C for 267 and 495 hours. After exposition surfaces of the test specimens were observed by scanning electron microscope. The results of quantitative evaluation of the exposed test specimens surfaces are summarized in tab. IV.

Tab. IV The results of quantitative evaluation of test specimens surfaces exposed in air at 275°Cfor 267 hours.

ε_{tot} of test spec.	Test spec. surface evaluated	Number of inclus. intersecting surface	Number of microcracks
0,2 %	52 mm^2	21	1
0,65 %	45 mm^2	10	2
1,7 %	45 mm^2	14	5

Longitudinal sections of the gage length of test specimen loaded to the total deformation of 1,7% revealed that nonmetallic inclusions of type $Ti_4C_2S_2$ and Ti(C,N) serves as preferential nucleation sites of microcracks. Microcracks are nucleated at 275°C already in air due to either mechanical failure of nonmetallic inclusion/matrix interface (see Fig. 3) or mechanical failure of nonmetallic inclusion (see Fig. 4).

Prolongation of exposition time from 267 hours to 495 hours had no effect on microcrack depth. The microcrack depth is dependent first of all on the inclusion size (0,01-0,03 mm).

The same microcracks were found near the surface of test specimen made from heat exchange tube and loaded to the total deformation of 0,35% after exposition for 495 hours in air at 275°C.

If the agressive environment and sufficient level of tensile stress are present microcracks nucleated on the surface by above mentioned mechanism can growth.

Another mechanism was observed on metallographic samples of test specimens exposed in deaerated acid solutions of Cl^- ions prepared from HCl. The microcracks were nucleated from the bottom of corrosion micropits observed on the fracture surfaces (see Fig. 5,6). The number of micropits is significantly dependent on concentration of Cl^- and high temperature pH of the solution. Fig.7 shows corrosion microcracks growing from both mechanically failured inclusions and from the micropits bottoms. Corrosion microcracks growing from failured inclusions intersecting the surface were found on test specimens exposed in deaerated acid solutions of SO_4^{2-} prepared from H_2SO_4 (see Fig. 8). The character of these microcracks differs significantly of those nucleated from micropits in acid solutions prepared from HCl.

Conclusions

Two mechanisms of corrosion microcracks nucleation were observed on the surfaces of test specimens made from 08X18N10T stainless steel:

1. Corrosion microcracks nucleated from the bottoms of micropits in acid solutions of Cl^-, $Cl^- + SO_4^{2-}$ and $Cl^- + SO_4^{2-} + Na^+$ (pH_{275} 1,7 – 2,3).
2. Corrosion microcracks nucleated from the mechanically failured interface nonmetallic inclusion/matrix, mechanically failured inclusions intersecting the surface and/or from imperfactions observed on the surface of heat exchange tubes in acid solutions (pH_{275} 1,8-4), and in alkaline solutions $pH_{275} > 9,0$.

References

[1] WOZNIAK,J.-MATOCHA,K.: Temperature and Strain Ageing of 08Kh18N10T Steel Initiated by Static and Dynamic Loading at Operating Temperature of Steam Generators. VÍTKOVICE-Research and Development Report , Z-6/98, Ostrava, March 1998 , (in Czech).

[2] MacDonald, P.E. at al.: Steam Generator Tube Failures (NUREG/CR – 6365, INEL – 95/0383, 1996) p.64

[3] Matocha, K.- Wozniak, J.- Pochman, K.: „Analysis of WWER 440 SG Primary Collector Bolted Joint Damage“ (In: Proc. of Fourth International Seminar on Horizontal Steam Generators, 11-13 March 1997, Laapeenranta, Fin.), p.148.

[4] MATOCHA,K.-WOZNIAK,J.: Stress Corrosion Cracking Initiation in Austenitic Stainless Steel in High Temperature Water. Ninth International Symposium on Environmental Degradation of Materials in Nuclear Power Systems-Water Reactors. Edited by F.P.Ford, S.M.Bruemmer and G.S. Was. The Minerals, Metals &Materials Society (TMS), 1999, p. 383.

[5] MATOCHA,K.-SMIEŠKO,I.-KOPŘIVA,M.-MARCINSKÝ,P.: The Effect of Water Impurities on Resistance of 08Kh18N10T (AISI321) Steel to SCC in High Temperature Water Environment. Proceedings of the Seventh International Conference on Material Issues in Design, Manufacturing and Operation of Nuclear Power Plants Eguipment, St.Petersburg, 17-21 June 2002, Vol.2., p.149.

[6] ASTM G 49 – 85, „Standard Practice for Preparation and Use of Direct Tension Stress – Corrosion Test Specimens“, Annual Book of ASTM Standards, Section 3, Vol.03.03, 1991, p.181

[7] Data Sheets on the Elevated Temperature Properties of 18Cr-8Ni-Ti Stainless Steel for Boiler and Heat Exchanger Seamless Tubes (SUS 321 HTB). NRIM Creep Data Sheet No. 5A,1978.

[8] MATOCHA,K.-HYSPECKÁ,L.-MAZANEC,K.: Low cycle fatigue of 08X18N10T welding joint . ZVÁRANIE, No.7,June 1989, p. 197, (in Czech).

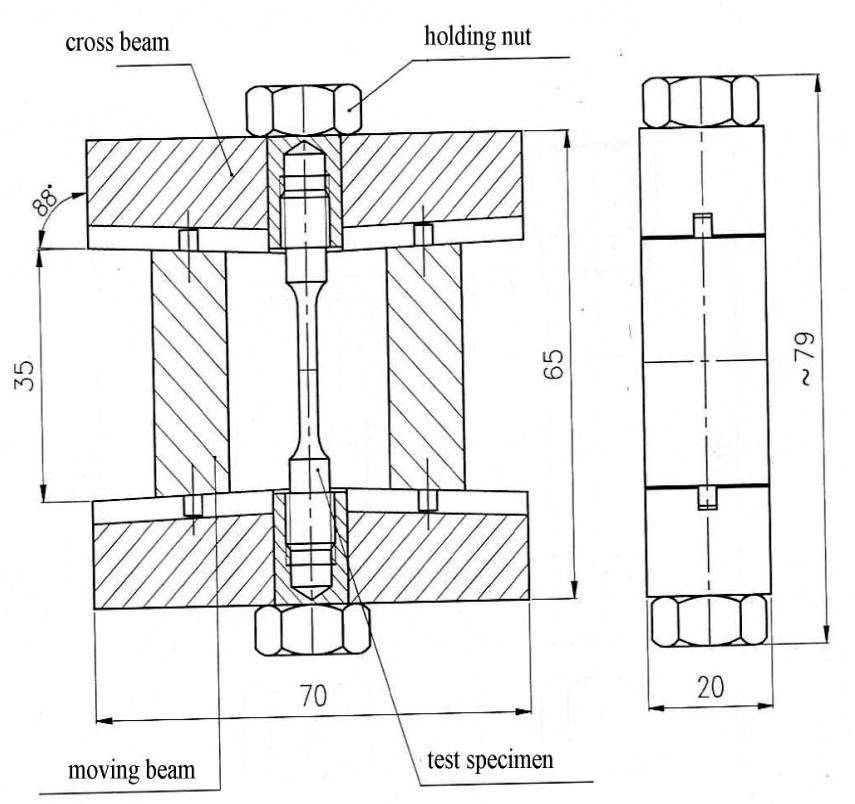

Fig.1 Dimensions of stressing frame according ASTM G 49-85 using for loading of round bar specimens, 3 mm in diameter.

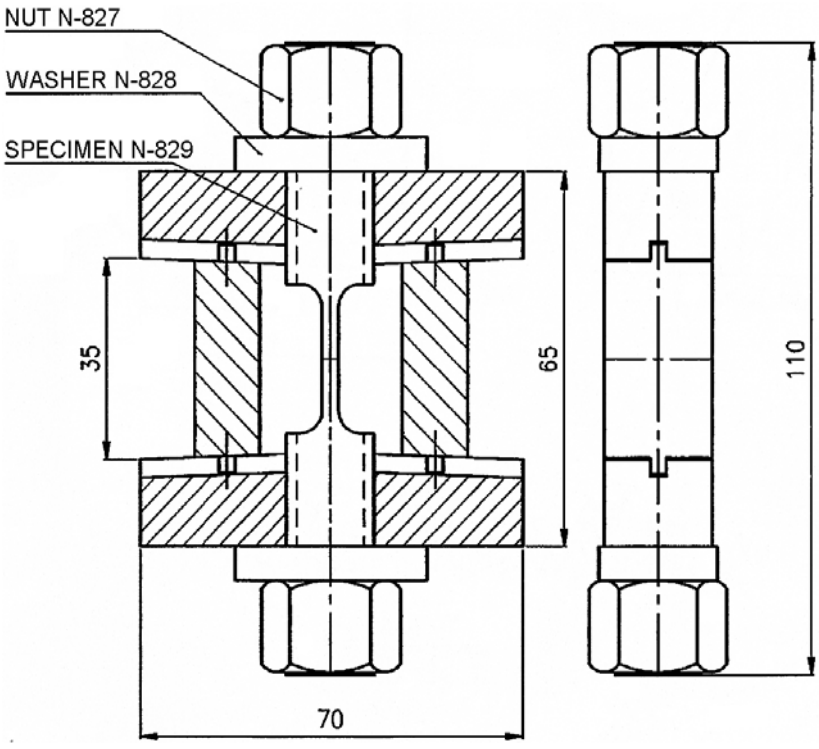

Fig.2 Dimensions of stressing frame according ASTM G 49-85 using for loading of special test specimens manufactured from heat exchanger tubes

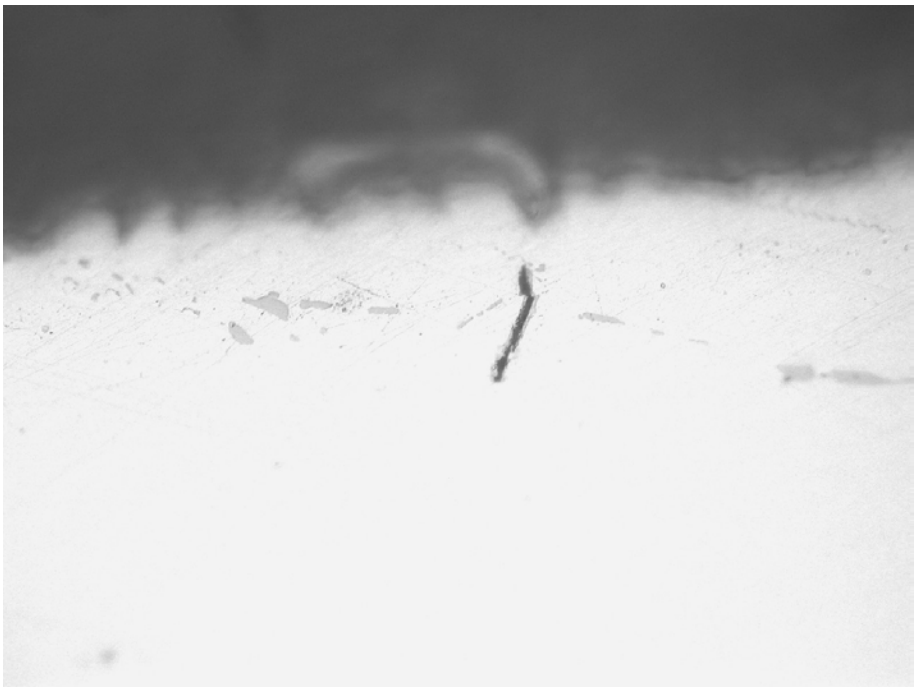

zv. 500x

Fig. 3 Mechanical failure of interface inclusion/matrix after loading in air at 275 °C, ε = 1,7 %, exposition time 267 hours (cylindrical specimen 3 mm in diameter)

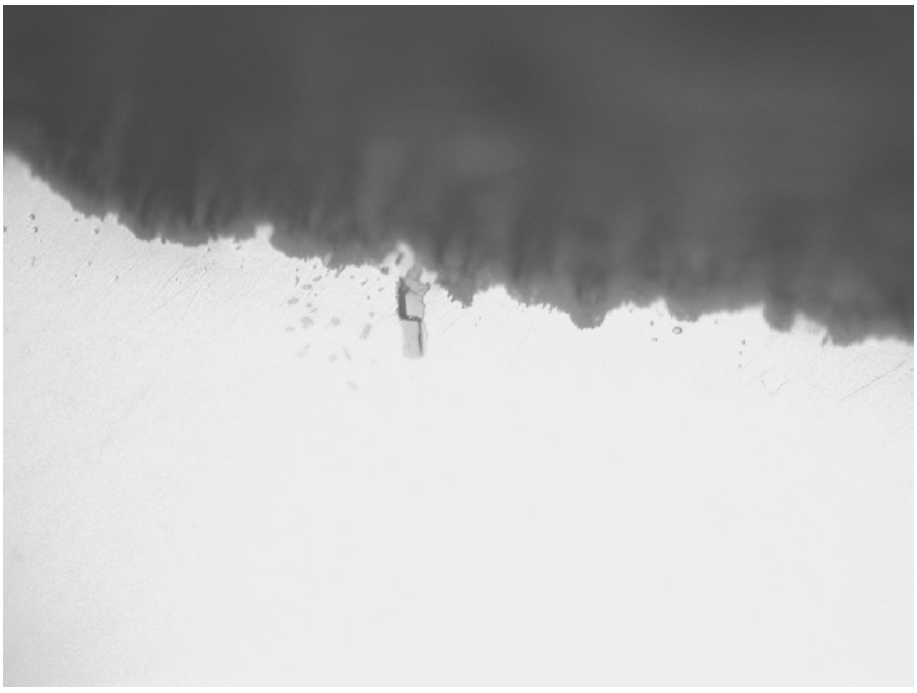

zv. 500x

Fig.4 Mechanical failure of inclusion (at matrix 08Ch18N10T) after loading in air at 275 °C, ε = 1,7 %, exposition time 495 hours (cylindrical specimen 3 mm in diameter).

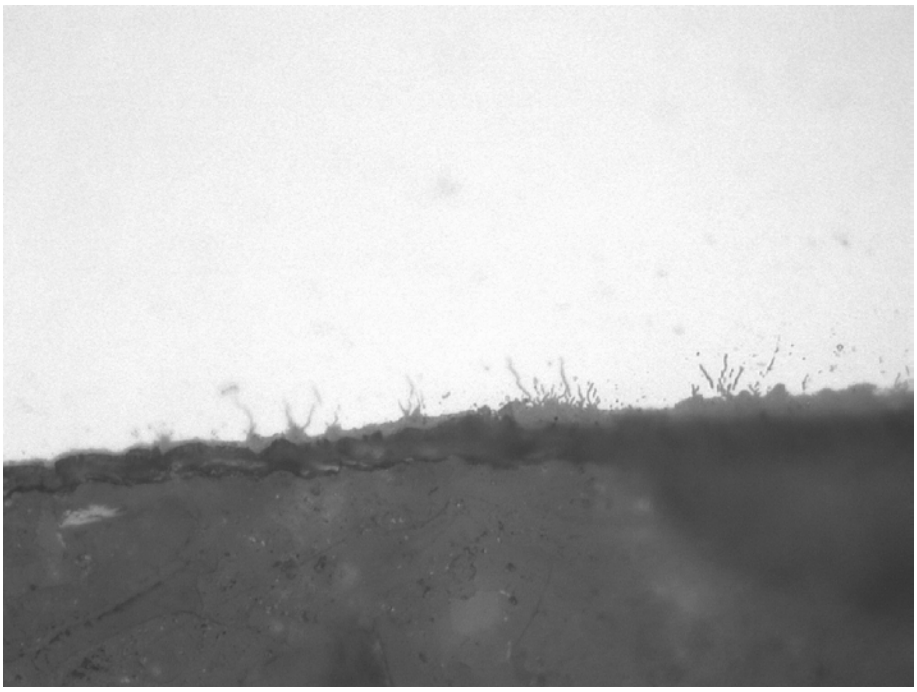

zv. 1000x

Fig.5 Microcracks nuclated from the bottoms of corrosion micropits on the surface of cylindrical specimen exposed in deaerated acid solution
100 ppm Cl^- prepared from HCl, pH_{275} 2,55, ε = 1,7 %, exposition time 240 hours

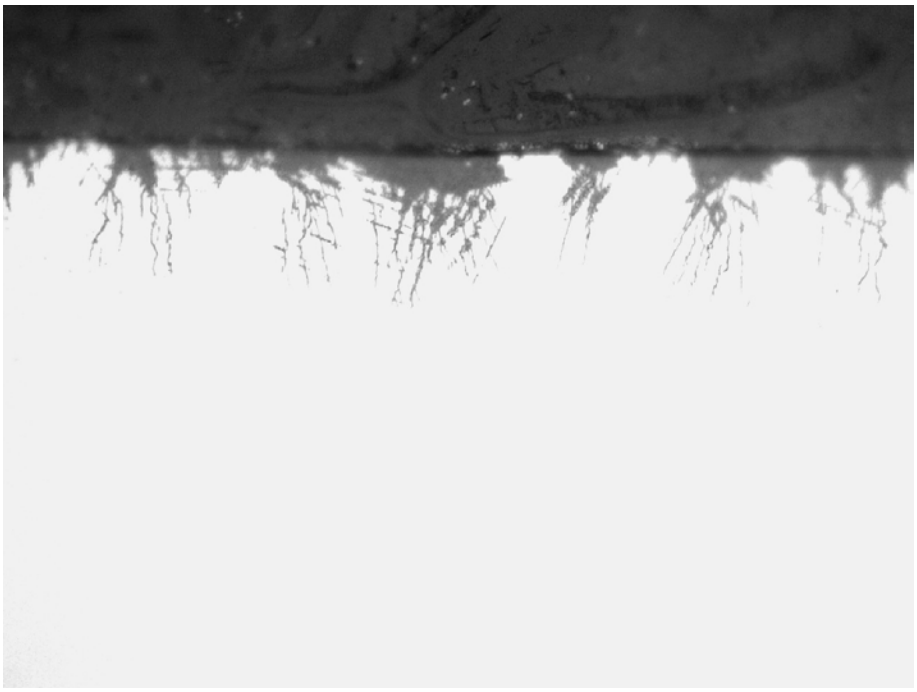

zv. 1000x

Fig.6 Microcracks nuclated from the bottoms of corrosion micropits on the surface of cylindrical specimen exposed in deaerated acid solution 500 ppm Cl^- prepared from HCl, pH pH_{275} 1,85, ε = 1,7 %, exposition time 240 hours

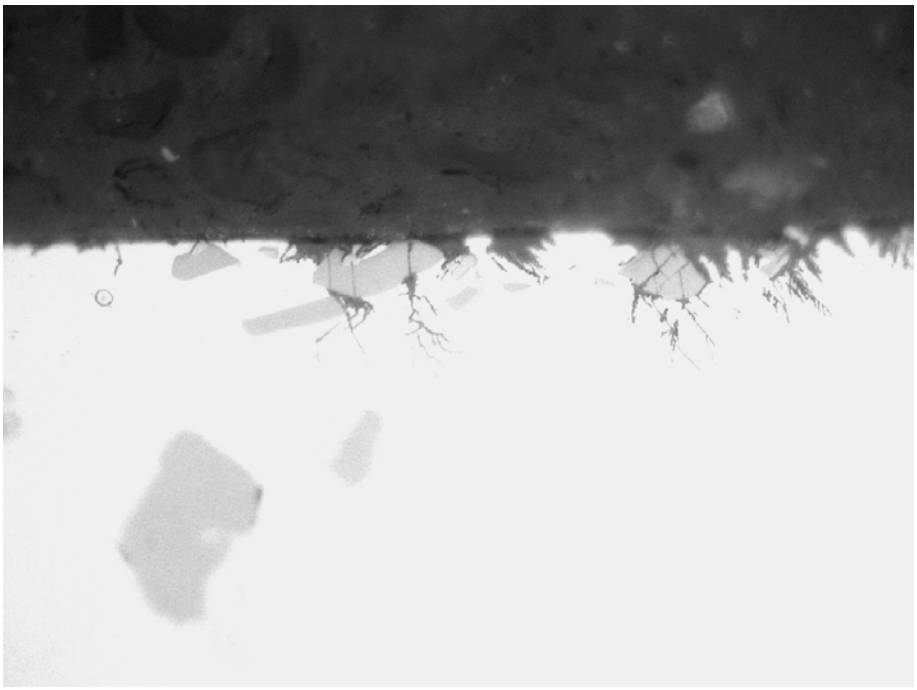

zv. 1000x

Fig.7 Corrosion microcracks nucleated both from mechanically failured inclusions and from the corrosion micropits bottoms of cylidrical specimen 3 mm in diameter, acid solution 500 Cl^- prepared from HCl, pH_{275} 1,85, ε = 1,7 %, exposition time 240 hours. temperature
t=275 °C

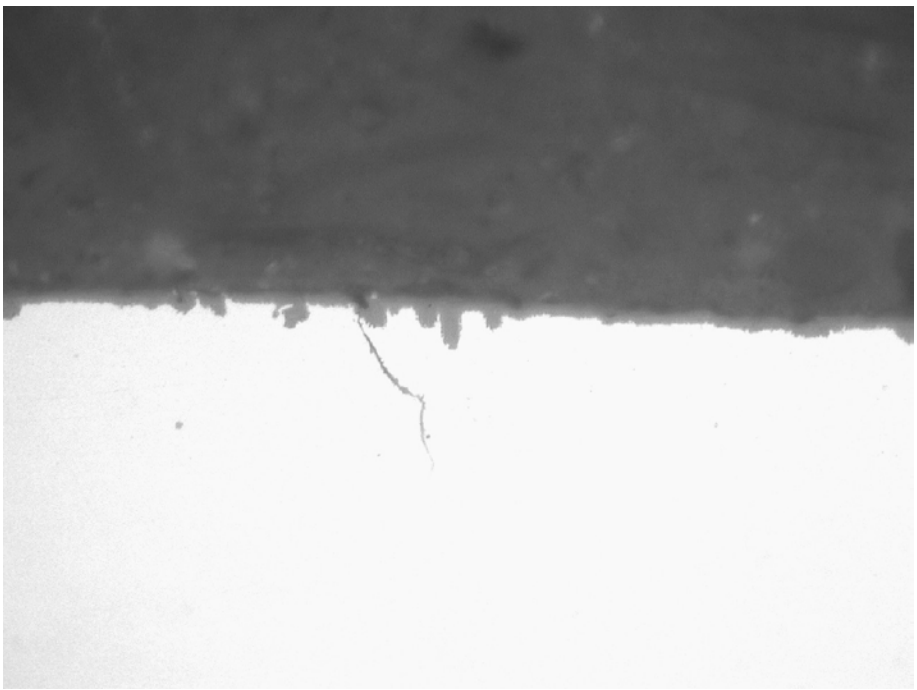

zv. 1000x

Fig.8 Corrosion microcrack found after exposition in deaerated acid solution 500 ppm SO_4^{2-} prepared from H_2SO_4, pH_{275} 2,28, ε = 1,7%, exposition time 240 hours, temperature t=275°C.